

## Galerkin Spectral Method Applied to the Chemical Master Equation

Stefan Engblom\*

*Department of Information Technology, Uppsala University, P. O. Box 337, SE-75105 Uppsala, Sweden.*

Received 11 March 2008; Accepted (in revised version) 23 July 2008

Communicated by Jan S. Hesthaven

Available online 29 September 2008

---

**Abstract.** Stochastic well-stirred chemically reacting systems can be accurately modeled by a continuous-time Markov-chain. The corresponding master equation evolves the system's probability density function in time but can only rarely be explicitly solved. We investigate a numerical solution strategy in the form of a spectral method with an inherent natural adaptivity and a very favorable choice of basis functions. Theoretical results related to convergence have been developed previously and are briefly summarized while implementation issues, including how to adapt the basis functions to follow the solution they represent, are covered in more detail here.

The method is first applied to a model problem where the convergence can easily be studied. Then we take on two more realistic systems from molecular biology where stochastic descriptions are often necessary to explain experimental data. The conclusion is that, for sufficient accuracy demands and not too high dimensionality, the method indeed provides an alternative to other methods.

**AMS subject classifications:** 65M70, 65C40, 60J22, 41A30, 41A63

**Key words:** Master equation, spectral-Galerkin method, high dimensional problem, moving basis, chemical reactions.

---

## 1 Introduction

Stochastic descriptions of chemical reactions are necessary tools for understanding and explaining the mechanisms inside living cells. Models of intra-cellular systems frequently consist of fewer than  $10^2$  molecules of some of the species [26] implying that molecule discreteness makes the impact of stochasticity very pronounced. For instance, randomness has been shown to drive and improve the regularity of oscillations [46], create new steady-states [45] and cause separation in bistable systems [13].

---

\*Corresponding author. *Email address:* stefane@it.uu.se (S. Engblom)

The *chemical master equation* (CME) is a popular and accurate stochastic model for chemically reacting systems. It is a consequence of the *Markov property*: if the system is measured at discrete times  $t_1 < t_2 < \dots < t_n$ , then the probability for the measurement  $(y_n, t_n)$  given the present state  $(y_{n-1}, t_{n-1})$  does not involve earlier states. Typically, because of the existence of activation energies, reactive collisions between molecules are rare events as compared to nonreactive ones giving rise to a randomization and a loss of memory [24]. This loss of memory is then accurately captured by the Markov property and remains a valid approximation so long as the measurement scale is slower than the often extremely short auto-correlation time of the system.

The master equation is a differential-difference equation in  $D$  dimensions, where  $D$  is the number of reacting agents, and is therefore a very computationally intensive problem. Effective numerical methods are of both practical and theoretical interest.

Recent progress at *directly* representing the state-space and solving the CME include the *Finite state projection algorithm* [38], later improved using Krylov-subspace methods [5,36]. See also [18] where techniques from adaptive PDE-solvers are used in the context of the CME. For larger state-spaces, numerical solution of the *Fokker-Planck equation* [19] and adaption of the *Sparse grids technique* [29] have been suggested. As a master equation for *continuous* stochastic processes, numerical solution of the Fokker-Planck equation is an interesting subject in itself. There are, however, important cases for which the CME cannot be approximated by the Fokker-Planck equation [22]. The sparse grids technique aims to reduce the computational complexity of high dimensional smooth problems. Its application to the CME is quite recent and appear promising.

In the present paper we implement and apply a spectral method developed previously in the report [17] to the master equation. The method employs basis functions that are orthogonal with respect to a discrete measure in line with the discreteness of the solution and avoids the need for continuous approximations to the master operator. An interesting feature of our implementation is a built-in adaptivity of the basis which allows the basis functions to follow the dynamical behavior of the solution. Our proposed scheme is reminiscent of an approach for polyreaction kinetics considered earlier in [9], and we will further comment on this point in Section 5.

The “curse of dimension”, the phenomenon that the complexity of traditional discretization methods applied to high-dimensional problems grows exponentially with the problem size is thus not removed, but it is mitigated. With a spectral method that converges exponentially, the resolution per dimension can be much smaller than any direct representation provided that the solution is smooth enough. As we shall see, another point in directly attacking the CME is the way stiff equations can be handled through suitable implicit time integration.

The paper is organized as follows. In Section 2 the master equation as a governing equation for stochastic chemical systems is discussed along with theoretical properties of importance to the numerical analysis. The spectral method is proposed in Section 3 where approximation and stability results developed in the report [17] are summarized. This section also discusses a plausible implementation in some detail, including the “moving

basis" technique. Section 4 is devoted to numerical experiments and investigates the performance of the method when applied to three different systems, two of which are representative from the field of molecular biology. The paper is concluded by discussing the various merits of the method and pointing to possible future considerations.

## 2 Background

As an introduction to the subject we devote this section to some theoretical and practical results. The first strict derivation of the CME as an exact description of well-stirred chemical reactions in thermal equilibrium occurred in [24]. Many properties, including extensions, of this equation of interest to the physicist are discussed in [20,31].

### 2.1 The master equation

We now let  $D$  different species react according to  $R$  prescribed reactions. In a stochastic description of this system, we let  $p(x,t)$  be the probability that a certain number  $x \in \mathbf{Z}_+^D = \{0,1,2,\dots\}^D$  of molecules is present at time  $t$ .

The reactions are now "jumps" between the states  $x$  with a certain jump intensity, or *reaction propensity*,  $w_r: \mathbf{Z}_+^D \rightarrow \mathbf{R}_+$ . This is the transition probability per unit of time for moving from the state  $x$  to  $x - \mathbb{N}_r$ ;

$$x \xrightarrow{w_r(x)} x - \mathbb{N}_r, \quad (2.1)$$

where by convention,  $\mathbb{N}_r \in \mathbf{Z}^D$  is the transition step and is the  $r$ th column in the *stoichiometric matrix*  $\mathbb{N}$ .

The *master equation* [20,31] is then given by

$$\begin{aligned} \frac{\partial p(x,t)}{\partial t} &= \sum_{\substack{r=1 \\ x+\mathbb{N}_r^- \geq 0}}^R w_r(x+\mathbb{N}_r)p(x+\mathbb{N}_r,t) - \sum_{\substack{r=1 \\ x-\mathbb{N}_r^+ \geq 0}}^R w_r(x)p(x,t) \\ &=: \mathcal{M}p, \end{aligned} \quad (2.2)$$

where the transition steps are decomposed into positive and negative parts as  $\mathbb{N}_r = \mathbb{N}_r^+ + \mathbb{N}_r^-$ .

As indicated, the summations are performed over *feasible* reactions only. In what follows, we shall only consider formulations where  $w_r(x) = 0$  whenever  $x \not\geq \mathbb{N}_r^+$ . This assumption is justified as follows (cf. [31, Ch. VII.2] and [20, Ch. 7.5]): let  $i$  be such that  $\mathbb{N}_{ri} > 0$ . Then  $w_r$  defines a certain reaction for which one or several  $x_i$ 's are annihilated. Obviously, this reaction cannot occur unless there are sufficiently many  $x_i$ 's left to annihilate and we therefore postulate that  $w_r$  is zero for  $x_i \in \{0,1,\dots,\mathbb{N}_{ri}-1\}$ .

Under this assumption, the *adjoint* operator  $\mathcal{M}^*$  has the following convenient representation [31, Ch. V.9]: if  $(p,q)$  is a pair of not necessarily normalized or positive functions

defined over  $\mathbf{Z}_+^D$ , then provided both sides make sense,

$$\mathcal{M}^*q = \sum_{r=1}^R w_r(x)[q(x - \mathbb{N}_r) - q(x)]. \quad (2.3)$$

If now  $X = [X_1, \dots, X_D]$  is the  $D$ -dimensional time-dependent stochastic variable for which  $p$  is the probability density function, then by taking the inner product with a suitable test-function  $T: \mathbf{Z}_+^D \rightarrow \mathbf{R}$  in (2.2) and using (2.3) we get

$$\frac{d}{dt}E[T(X)] = \sum_{r=1}^R E[(T(X - \mathbb{N}_r) - T(X))w_r(X)]. \quad (2.4)$$

Using this form of the adjoint, equations for the various moments of  $X$  can be formed (see [15] for a numerical investigation of this approach). In fact, the most common deterministic approach corresponds to  $T(x) = x$  and gives, upon ignoring higher order moments, the *reaction-rate* equations. This is a set of  $D$  ordinary differential equations (ODEs) approximating the expected values of the species in the system. There are, however, many systems for which the reaction-rate equations either fail to reproduce the observed dynamics [42] or are less meaningful.

The CME is equivalent to a continuous-time Markov chain in the stochastic variable  $X$ :

$$X_{k+1} = X_k + \mathbb{N}e_m, \quad (2.5)$$

$$t_{k+1} = t_k + \tau_k, \quad (2.6)$$

where  $e_m$  is the  $m$ th unit vector chosen according to the prescription

$$\Pr[m = r] = \alpha w_r(X_k), \quad (2.7)$$

where

$$\alpha \equiv \left( \sum_{r=1}^R w_r(X_k) \right)^{-1}, \quad (2.8)$$

and where the time-step  $\tau_k$  is drawn from an exponential distribution with mean  $\alpha$ . This formulation is equivalent to *Gillespie's Stochastic Simulation Algorithm* (SSA) [23] and offers the ability to *exactly* follow sample trajectories of the system. For systems where the number of reactions to be simulated is very large, SSA becomes inefficient since it follows the system in complete detail. For this purpose, the *tau-leap method* [25] was developed and later improved [2] and analyzed [33,41].

Although simulating one trajectory can be performed relatively fast for many systems, models in molecular biology are often very stiff and therefore expensive to solve by

explicitly simulating the various time-scales. As a remedy, model reduction techniques have been proposed [6, 12, 27]. The tau-leap method can be regarded as an instance of the forward Euler method [33] and as such is not a good alternative for stiff problems. An implicit version has therefore been developed [40], but this method converges in a very weak sense only [7, 34, 41].

## 2.2 Solution properties

If  $(\lambda, q)$  is an eigenpair of  $\mathcal{M}^*$  normalized so that the largest value of  $q$  is positive and real, then we see from (2.3) that  $\Re\lambda \leq 0$  so that the eigenvalues of  $\mathcal{M}$  also have this property. Since generally,  $\mathcal{M}$  is not a normal operator, this does not imply that the  $l^2$ -norm cannot increase with time. However, from the fact that the semigroup corresponding to  $\mathcal{M}$  is contractive (see [11, Ch. 1]), this stability property holds provided that the  $l^1$ -norm is used instead:

**Theorem 2.1.** *Let the initial data  $p(x,0)$  be a not necessarily normalized or positive, but  $l^1$ -measurable function. Then any solution to the master equation is non-increasing in the  $l^1$ -sequence norm. That is,*

$$\sum_{x \geq 0} |p(x,t)| \leq \sum_{x \geq 0} |p(x,0)| \quad (2.9)$$

for any  $t \geq 0$ .

We also consider the steady-state limit  $t \rightarrow \infty$  and start by giving two preliminary definitions. A *decomposable* linear operator can be cast in the form (by relabeling the states)

$$\mathcal{M} = \begin{bmatrix} \mathcal{M}_{11} & 0 \\ 0 & \mathcal{M}_{22} \end{bmatrix}, \quad (2.10)$$

while a *splitting* operator can be written as

$$\mathcal{M} = \begin{bmatrix} \mathcal{M}_{11} & \mathcal{M}_{12} & 0 \\ 0 & \mathcal{M}_{22} & 0 \\ 0 & \mathcal{M}_{32} & \mathcal{M}_{33} \end{bmatrix}. \quad (2.11)$$

Master operators of this form are not fully connected and essentially consist of multiple isolated subsystems.

**Theorem 2.2.** *Let  $p(x,0)$  be an  $l^1$ -measurable discrete function defined on  $\mathbf{Z}_+^D$  and let  $\mathcal{M}$  be neither decomposable nor a splitting. Then the master equation (2.2) admits a unique steady-state solution as  $t \rightarrow \infty$ . Moreover, if  $p(x,0)$  is a discrete probability density, then so is the steady-state solution.*

For a proof with many references and a thorough discussion we refer the reader to [31, Ch. V.3]. Formally, the result is only valid when the number of states is finite. For master equations describing physical systems, however, the number of states must obviously be bounded. We therefore expect reasoning based on assuming a finite number of states to be valid for all physically realizable systems.

We consider finally the linear birth-death process [3] as a model problem in one dimension:



where conventionally we use uppercase letters to denote molecule *names*, while lower-cases are used for counting the number of molecules. Eq. (2.12) states that  $X$ -molecules are added to the system at constant rate and depleted at a rate proportional to the total number of molecules. The corresponding CME can be written in terms of the forward- and backward difference operator  $\Delta q(x) = q(x+1) - q(x)$  and  $\nabla q(x) = q(x) - q(x-1)$ ,

$$\frac{\partial p(x,t)}{\partial t} = \mathcal{M}p(x,t) = -k\bar{\nabla} p(x,t) + \mu\Delta[xp(x,t)], \quad (2.13)$$

where we use a bar over  $\nabla$  to express the convention that  $p(-1,t) = 0$ . This problem can be solved analytically if initial data is given in the form of a Poissonian distribution of expectation  $a_0$ ,

$$p(x,0) = \frac{a_0^x}{x!} e^{-a_0}. \quad (2.14)$$

The full dynamic solution is

$$p(x,t) = \frac{a(t)^x}{x!} e^{-a(t)}, \quad (2.15)$$

where  $a(t) = a_0 \exp(-\mu t) + k/\mu \cdot (1 - \exp(-\mu t))$ . Evidently, the steady-state distribution is a Poissonian distribution with expectation  $k/\mu$ .

The analytical solution in this example is a partial motivation for the choice of basis functions in the next section. *Charlier's* polynomials are orthogonal with respect to the Poisson process and seems to be natural candidates for representing solutions to the master equation.

### 3 A discrete spectral method

Spectral Galerkin methods are generally considered to be efficient solution strategies for linear time-dependent problems in the absence of difficult geometries [30]. For *stochastic*

*differential equations* (SDEs), *stochastic Galerkin methods* [37, 49, 50] have been devised for many types of equations, but the direct application of spectral methods to the CME is more recent. In contrast to most SDEs from applications, which are often derived by adding noise to a deterministic description, the CME follows from first principles and is a consequence of the Markov assumption only.

### 3.1 Approximation of functions on $\mathbf{Z}_+$

A theory for the approximation of functions defined on  $\mathbf{Z}_+$  was developed in the report [17] and we summarize our findings in this section. The main result is Theorem 3.1 which states that, given sufficient regularity in the solution to the CME, there is a certain basis in which the error rapidly decays with increasing resolution. Expanding smooth solutions to the CME in this basis thus reduces the number of degrees of freedom substantially.

For  $p \in \{1, 2, \infty\}$ , we use the normed  $l^p(\mathbf{Z}_+)$ -spaces,

$$l^p(\mathbf{Z}_+) = \left\{ q: \mathbf{Z}_+ \rightarrow \mathbf{R}; \|q\|_{l^p(\mathbf{Z}_+)} < \infty \right\}, \quad (3.1)$$

$$\|q\|_{l^p(\mathbf{Z}_+)}^p \equiv \sum_{x \geq 0} |q(x)|^p, \quad (3.2)$$

where the usual sup-norm is to be understood when  $p = \infty$ . For  $p = 2$  we additionally associate the discrete Euclidean inner product,

$$(p, q) \equiv \sum_{x \geq 0} p(x)q(x). \quad (3.3)$$

Define now the falling factorial function by  $x^{\underline{m}} = \prod_{i=0}^{m-1} (x-i)$  along with the following hierarchy of parameterized discrete Sobolev-spaces:

$$h^m(\mathbf{Z}_+) = \left\{ q: \mathbf{Z}_+ \rightarrow \mathbf{R}; \|q\|_{h^m(\mathbf{Z}_+)} < \infty \right\}, \quad (3.4)$$

$$\|q\|_{h^m(\mathbf{Z}_+)}^2 \equiv \sum_{k=0}^m a^{-k} \|\sqrt{x^{\underline{k}}} \cdot q(x)\|_{l^2(\mathbf{Z}_+)}^2, \quad (3.5)$$

and where the choice of the parameter  $a \in \mathbf{R}_+$  will be discussed in Section 3.3.

We first note the evident boundedness of the operation multiplication by a polynomial which follows from the definition (3.5):

**Proposition 3.1.** The map  $F: h^{m+2n}(\mathbf{Z}_+) \rightarrow h^m(\mathbf{Z}_+)$  defined by  $F(q) = x^n \cdot q(x)$  is continuous.

The following result was proved in [17, Report] and can be used together with Proposition 3.1 to bound the regularity of quite general master operators. Recall from (2.13) that  $\bar{\nabla} p(x) \equiv p(x-1) - p(x)$  with the exception of  $\bar{\nabla} p(0) \equiv -p(0)$ .

**Proposition 3.2.** The maps  $\bar{\nabla}: h^m(\mathbf{Z}_+) \rightarrow h^m(\mathbf{Z}_+)$  and  $\Delta: h^m(\mathbf{Z}_+) \rightarrow h^m(\mathbf{Z}_+)$  are continuous.

We can also define *weighted* Sobolev-spaces with weight  $w(x) = a^x / x! \cdot e^{-a}$ . The inner product is then

$$(p, q)_w \equiv \sum_{x \geq 0} p(x)q(x)w(x) \quad (3.6)$$

with generated norm  $\|\cdot\|_{l_w^2}$ . In analogy to (3.4) and (3.5) we can extend this to a hierarchy of weighted spaces  $h_w^m$ . The rationality behind this construction is that the two hierarchies of Sobolev-spaces  $h_w^m$  and  $h^m$  are connected through the *isomorphism*  $p \rightarrow w^{1/2}p$ , implying that approximation results in  $h_w^m$  carry over to  $h^m$ .

Denote by  $C_n^a(x)$  the *normalized*  $n$ th degree Charlier polynomial [32, Report] with parameter  $a > 0$ . These polynomials form an orthonormal set of functions with respect to the  $l_w^2$ -product;  $(C_n^a, C_m^a)_w = \delta_{nm}$ . Write  $X_N$  for the span of the (Charlier-) polynomials of degree  $\leq N$  and define  $\pi_N$  as the orthogonal projection onto  $X_N$  associated with  $(\cdot, \cdot)_w$ .

The normalized Charlier polynomials satisfy the recurrence

$$\begin{aligned} C_0^a(x) &\equiv 1, \\ C_1^a(x) &\equiv \frac{a-x}{\sqrt{a}}, \\ C_{n+1}^a(x) &= \frac{n+a-x}{\sqrt{a(n+1)}} C_n^a(x) - \sqrt{\frac{n}{n+1}} C_{n-1}^a(x), \end{aligned} \quad (3.7)$$

and they also obey the interesting relation

$$C_n^a(x) = (-1)^n \sqrt{\frac{n!}{a^n}} L_n^{x-n}(a), \quad (3.8)$$

where  $L_n^a$  denote *Laguerre polynomials* [32, Report] with the usual normalization.

Furthermore, define *Charlier's functions* by  $\hat{C}_n^a(x) := C_n^a(x) \cdot w(x)^{1/2}$  along with the space

$$\hat{X}_N = \{p(x) = q(x) \cdot w(x)^{1/2}; q \in X_N\}.$$

Evidently, these functions are orthonormal under the usual  $l^2$ -product  $(\cdot, \cdot)$  and we use  $\hat{\pi}_N$  to denote the corresponding orthogonal projection on  $\hat{X}_N$ .

We quote from [17, Report] the following approximation result.

**Theorem 3.1.** For any nonnegative integers  $k$  and  $m$ ,  $k \leq m$ , there exists a positive constant  $C$  depending only on  $m$  and  $a$  (or only on  $m$  provided  $a \geq 1$  is given) such that, for any function  $p \in h^m(\mathbf{Z}_+)$ , the following estimate holds

$$\|\hat{\pi}_{N-1}p - p\|_{h^k(\mathbf{Z}_+)} \leq C(a/N)^{m/2} \max(1, N/a)^{k/2} \|p\|_{h^m(\mathbf{Z}_+)}. \quad (3.9)$$

Theorem 3.1 is related to similar results for continuous approximation; see for example [43].

There are several reasons for why the space  $\hat{X}_N$  is preferred to  $X_N$  when seeking approximations to solutions of the master equation. First, any Galerkin formulation in the inner product  $(\cdot, \cdot)_w$  will at best lead to convergence in the weighted norm  $\|\cdot\|_{L_w^2}$ . In contrast, a convergent Galerkin formulation in the  $l^2$ -product implies the existence of error estimates in the much stronger  $l^2$ -norm. Second, solutions in  $X_N$  are not probability distributions and statistical measures of interest, such as the mean and variance, can not be defined.

### 3.2 Conservation and stability

A nuisance with the projection  $\hat{\pi}_N$  is that it does not preserve the probability mass; since the constant function  $1 \notin l^2(\mathbf{Z}_+)$  we expect in general that  $(1, \hat{\pi}_N p) \neq (1, p) = 1$ . A remedy is devised in [17, Report]; consider the projection  $\hat{\pi}_N^0 p = p_N$  which for some Lagrange multiplier  $\lambda$  satisfies

$$\left. \begin{aligned} (q, p_N - p) + \lambda(f(q), 1) &= 0 \\ (1, p_N - p) &= 0 \end{aligned} \right\} \text{ for } \forall q \in \hat{X}_N, \tag{3.10}$$

where  $f$  is a linear function. For instance, the ‘‘tau-method’’ [30] of enforcing boundary conditions in spectral methods would be equivalent to the choice  $f(q) = (\hat{C}_N^a, q) \hat{C}_N^a$ . It is shown in [17, Report] that the tau-projection performs worse than the convenient choice  $f(q) = \hat{\pi}_0 q$ . This choice satisfies the bounds

$$\|\hat{\pi}_N^0 p - p\|_{l^2} \leq \|\hat{\pi}_N p - p\|_{l^2} + \frac{|(1, \hat{\pi}_N p - p)|}{(1, \hat{C}_0^a)}, \tag{3.11}$$

$$\|\hat{\pi}_N^0 p - p\|_{l^1} \leq \|\hat{\pi}_N p - p\|_{l^1} + |(1, \hat{\pi}_N p - p)|. \tag{3.12}$$

Note that  $|(1, \hat{\pi}_N p - p)|$  is the probability mass lost by  $\hat{\pi}_N$  which we expect to decay exponentially with  $N$ . Hence the additional error in either one of (3.11) or (3.12) is at worst proportional to this quantity. An asymptotic expression for the denominator in (3.11) when  $a$  is large is given in (3.17) below.

Consider now the stability properties of the Galerkin approximation to the CME (2.2) according to (3.10). The formulation is as follows: find  $p_N \in \hat{X}_N$  such that

$$\left. \begin{aligned} (q, \partial p_N / \partial t) + \lambda(\hat{\pi}_0 q, 1) &= (q, \mathcal{M} p_N) \\ (1, \partial p_N / \partial t) &= 0 \end{aligned} \right\} \text{ for } \forall q \in \hat{X}_N. \tag{3.13}$$

Since  $\mathcal{M}$  generally is unbounded, indefinite and non-symmetric with non-orthogonal eigenvectors, we cannot hope to capture the stability properties of (3.13) by any standard energy estimates. In [17, Report] some partial results were presented based on observations due to van Kampen [31, Ch. V] and Theorem 2.1. A short summary of these findings now follows.

The derivative of the  $l^1$ -norm can be written down explicitly:

$$\frac{d}{dt} \|p_N\|_{l^1} = \underbrace{\sum_{x \geq 0} \text{sgn } p_N \mathcal{M} p_N}_{=: A_N} + \underbrace{\sum_{x \geq 0} \text{sgn } p_N [\hat{\pi}_N^0 \mathcal{M} p_N - \mathcal{M} p_N]}_{=: B_N}, \tag{3.14}$$

where  $\text{sgn } q$  is zero for  $q = 0$ . It is not difficult to see that we *always* have that  $A_N \leq 0$ . Furthermore, if  $\mathcal{M}$  is not decomposable nor a splitting (cf. (2.10) and (2.11)) and  $B_N$  does not vanish, then the strict inequality  $A_N < 0$  holds. In conclusion, the only cases which could induce an increase in the  $l^1$ -norm occurs when  $B_N > |A_N|$ . Assuming sufficient regularity on  $\mathcal{M}$ ,  $B_N$  will tend rapidly to zero with increasing  $N$ . Hence the coercivity-type bound

$$|A_N| \geq \kappa(\mathcal{M}) \|\mathcal{M} p_N\|_{l^1}$$

would suffice to prove strict stability in  $l^1$ .

This argument does not strictly prove  $l^1$ -stability unless the coercivity estimate is first proved but it does shed some light on the expected stability properties. Also, the nice representation (3.14) is due to the mass-preserving projection and thus indicates why this is a favorable choice.

### 3.3 Adaptivity

We now pay attention to the choice of the parameter  $a$  which must be chosen prior to forming any projection onto  $\hat{X}_N$ . We examine a simplified case and claim that *if  $N$  is small and  $p$  is a “one-peak” probability distribution with expectation value  $m$ , then  $a \approx m - 1/2$  is close to optimal*. By a “one-peak” probability distribution we mean a unimodal distribution with standard deviation relatively small compared to the expectation value. Admittedly, solutions to the CME are not always one-peak distributions but we use this setting to get some guidance.

To motivate the statement we consider the case  $N = 0$  which means that  $p$  is to be approximated by the “half Poissonian distribution”,

$$P^{1/2}(x;a) = C^{-1} \hat{C}_0^a(x) = C^{-1} \sqrt{\frac{a^x}{x!}} e^{-a}. \tag{3.15}$$

Here  $C$  is the normalizing constant given by

$$C = \sum_{x \geq 0} \sqrt{\frac{a^x}{x!}} e^{-a} = \sum_{x \geq 0} \frac{(a/2)^x}{x!} e^{-a/2} f(x), \tag{3.16}$$

where

$$f(x) = \pi^{1/4} \sqrt{\frac{\Gamma(x+1)}{\Gamma(x+1/2)}} \left( 1 + \sqrt{\frac{a}{2x+1}} \right),$$

where  $\Gamma(x+1) = x!$  is the gamma function [1] and where the last line follows from summing even and odd terms separately and using Legendre's duplication formula [1]. To evaluate the sum in (3.16), we note that it can be compactly written as  $E[f(X)]$  for  $X$  a Poissonian stochastic variable of expectation  $a/2$ . Expand  $f$  in a Taylor series around  $a/2$  and assume  $a$  to be large so that Stirling's expansion [1] for the gamma function applies. Inserting formulas for the central moments of the Poissonian distribution then yields after some work,

$$C \sim 2^{3/4} \pi^{1/4} a^{1/4} \left( 1 - \frac{1}{16a} + \mathcal{O}(a^{-2}) \right). \quad (3.17)$$

Proceeding similarly for the expectation value  $m$  and the variance  $\sigma^2$  we obtain

$$m \sim a + \frac{1}{2} + \frac{1}{8a} + \mathcal{O}(a^{-2}), \quad (3.18)$$

$$\sigma^2 \sim 2a - \frac{1}{4a} + \mathcal{O}(a^{-2}). \quad (3.19)$$

The method just described for obtaining these expressions is somewhat related to the method of Laplace [39] in the theory of asymptotic expansions of integrals. Interestingly, it can also be shown to be equivalent to a technique due to Ramanujan (see [4], Ch. 3, entry 10). The resulting formulas are surprisingly accurate already for quite small values of  $a$ . For example, the indicated three terms in (3.18) yield a relative error less than 0.06% even for  $a=2$ . Taken together, (3.18) and (3.19) show that  $P^{1/2}$  is situated slightly to the right of a Poisson distribution with the same parameter and is about 41% wider.

In conclusion then, if the probability distribution  $p$  is reasonably centered around its expectation value  $m$ , then we expect that the optimal approximation in  $\hat{X}_0$  is nearly  $P^{1/2}(x; m-1/2)$  in (3.15). As  $N$  grows and the approximating space gets larger, this estimate no longer holds true. By Theorem 3.1 we see that  $a$  should reasonably decrease for the error to rapidly become small. We resort to a small informative experiment.

In Fig. 1 the  $l^2$ -error induced by projecting a *fix* Poisson distribution onto  $\hat{X}_N$  using different  $a$ 's and  $N$ 's are shown together with the optimal choice of  $a$  thus determined. The behavior of the optimal value  $a_{opt}$  is found to agree with the above discussion; for small  $N$  we see that  $a_{opt}$  is slightly less than the expectation value, while it decreases with increasing order  $N$ . We note that the *global* trend of the error near the optimal value is quite flat so that the precise choice is not so important. The oscillating *local* behavior of the error can be explained by considering asymptotic expansions for the Charlier polynomials in terms of Bessel functions (see [10] for this fairly complicated issue).

### 3.4 Implementation

In this section we will describe the suggested numerical scheme in some detail. The assembly process is discussed and we also demonstrate a feasible way to continuously

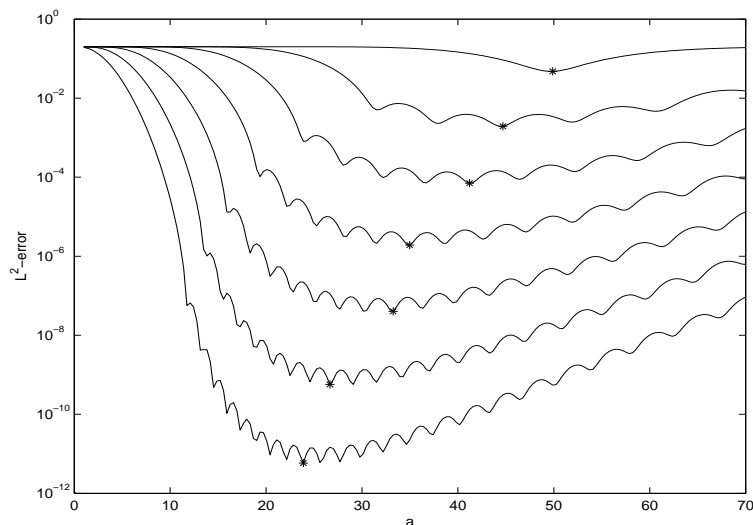


Figure 1: A Poisson distribution of expectation value 50 is projected on  $\hat{X}_N$  for  $N=0,5,\dots,30$  using several values of  $a$ . The  $l^2$ -error is determined for each choice of  $a$  producing the dependence shown. For each value of  $N$ , the asterisk indicates the optimal value of  $a$ .

update the parameter  $a$  so as to allow the basis functions to capture the dynamics of the solution.

Since the master operator is defined in  $D$  dimensions, we need to make use of multi-indices which we denote by small Greek letters. If  $\alpha=[\alpha_1,\dots,\alpha_D]$  and  $x$  is a  $D$ -dimensional array, then we index  $x$  by

$$x_\alpha = x_{\alpha_1,\dots,\alpha_D}. \tag{3.20}$$

In addition, the following products occur naturally,

$$\beta^\alpha = \beta_1^{\alpha_1} \dots \beta_D^{\alpha_D}, \tag{3.21}$$

$$\alpha! = \alpha_1! \dots \alpha_D!, \tag{3.22}$$

$$e^\alpha = e^{\alpha_1} \dots e^{\alpha_D}. \tag{3.23}$$

The easiest way of constructing a basis in  $D$ -dimensions is to use a tensor basis. We thus write

$$\hat{C}_\gamma^a(x) \equiv \prod_j \hat{C}_{\gamma_j}^{a_j}(x_j). \tag{3.24}$$

Evidently, this system of polynomials is orthonormal with respect to the inner product

$$(f,g) \equiv \sum_{x \geq 0} f(x)g(x) \prod_j \frac{a_j^{x_j}}{x_j!} e^{-a_j} = \sum_{x \geq 0} f(x)g(x) \frac{a^x}{x!} e^{-a}, \tag{3.25}$$

where  $x$  and  $a$  now are vector quantities. The solution to the CME is thus represented compactly as

$$p(x,t) = \sum_{\gamma} c_{\gamma}(t) \hat{C}_{\gamma}^a(x). \quad (3.26)$$

Multiplying both sides of the CME (2.2) by  $\hat{C}_{\delta}^a$  and summing over  $\mathbf{Z}_+^D$  yields the set of equations

$$\begin{aligned} c'_{\delta} &= (\hat{C}_{\delta}^a, \mathcal{M}p) = (\mathcal{M}^* \hat{C}_{\delta}^a, p) \\ &= \sum_{r=1}^R \sum_{\gamma} \left( C_{\delta}^a(x - \mathbf{N}_r) \cdot \sqrt{a^{-\mathbf{N}_r} x! / (x - \mathbf{N}_r)!} - C_{\delta}^a(x), w_r(x) c_{\gamma} C_{\gamma}^a(x) \right), \end{aligned} \quad (3.27)$$

where the favorable representation of the adjoint has been used. The use of orthogonality to simplify the above expression is notationally non-trivial but computationally quite simple. What is left is  $R$  different sums to be performed over the dimensions involved in each reaction; i.e. the dimensions  $i$  such that  $w_r$  depends on  $x_i$  and/or  $\mathbf{N}_{ri}$  is non-zero. *The number of dimensions in each sum is almost always bounded by 4.* For example, this is the case with the reaction  $x + y \rightarrow z$  with propensity  $w(x,y,e)$ . That is, when two species interact under the influence of an enzyme  $e$ .

The sums themselves are computed using an associated *Gauss-Charlier quadrature* [16, Report]. In one dimension it is given by

$$\sum_{x \geq 0} f(x) \frac{a^x}{x!} e^{-a} = \sum_{j=1}^n f(x_j) w_j + R_n, \quad (3.28)$$

$$R_n = a^n n! \frac{f^{(2n)}(\xi)}{(2n)!}, \quad \xi \in (0, \infty). \quad (3.29)$$

The  $x_j$ 's are the roots of  $C_n^a(x)$  and the weights can be computed according to the formula

$$w_j = -(an)^{-1/2} / [C_{n-1}^a(x_j) \cdot d/dx C_n^a(x_j)].$$

The quadrature provides a finite approximation to the Poisson distribution in the form

$$\Pr[x] = \sum_{j=1}^n w_j \delta_{x_j}(x), \quad (3.30)$$

where  $\delta_y(x) = 1$  if  $y = x$  and zero otherwise. In fact, the density in (3.30) has the same first  $2n$  moments as the corresponding Poisson distribution; for a fix parameter  $a$  and  $n \rightarrow \infty$  we thus have that  $x_j \sim j-1$  and  $w_j \sim w(x_j)$ .

Turn now to a discussion of the interesting and novel strategy of dynamically adapting the parameter  $a$ . Intuitively, the basis is most "active" in a neighborhood of  $x \sim a$ , and consequently we would like to adjust  $a$  so as to rapidly capture the behavior of the

represented solution. A different but related viewpoint is that the quadrature points tend to be more densely populated around  $a$  and we would like to ensure that no quadrature points are “wasted”.

Accordingly, let  $a = a(t) = [a_1(t), \dots, a_D(t)]$  in (3.26). Then formally,

$$\frac{\partial p(x,t)}{\partial t} = \sum_{\gamma} c'_{\gamma} \hat{C}_{\gamma}^a(x) + \sum_{\gamma} \left( \frac{a'}{C_{\gamma}^a(x)} \frac{d}{da} C_{\gamma}^a(x) + \frac{x a'}{2a} - \frac{a'}{2} \right) c_{\gamma} \hat{C}_{\gamma}^a(x), \tag{3.31}$$

which is just the product rule for derivatives. From (3.8) and a formula for the derivative of the Laguerre polynomials [1],

$$\frac{d}{dx} L_n^a(x) = -L_{n-1}^{a+1}(x), \tag{3.32}$$

one readily gets in the scalar case,

$$\frac{d}{da} C_n^a(x) = -\frac{n}{2a} C_n^a(x) + \sqrt{\frac{n}{a}} C_{n-1}^a(x). \tag{3.33}$$

Inserting this and using the recurrence (3.7), one can simplify the derivative, thereby finding

$$\begin{aligned} \frac{\partial p(x,t)}{\partial t} = & \sum_{\gamma} c'_{\gamma} \hat{C}_{\gamma}^a(x) \\ & + \sum_{\gamma} c_{\gamma} \sum_j \hat{C}_{\gamma \setminus \gamma_j}^{a \setminus a_j}(x \setminus x_j) \left( -\frac{1}{2} \sqrt{\frac{\gamma_j+1}{a_j}} \hat{C}_{\gamma_{j+1}}^{a_j}(x_j) + \frac{1}{2} \sqrt{\frac{\gamma_j}{a_j}} \hat{C}_{\gamma_{j-1}}^{a_j}(x_j) \right) a'_j. \end{aligned} \tag{3.34}$$

Here we had to be able to remove dimensions from the product — the precise meaning of the above notation is simply

$$\hat{C}_{\gamma \setminus \gamma_j}^{a \setminus a_j}(x \setminus x_j) \equiv \prod_{i \neq j} \hat{C}_{\gamma_i}^{a_i}(x_i). \tag{3.35}$$

It follows that

$$\left( \hat{C}_{\delta}^a, \frac{\partial p(x,t)}{\partial t} \right) = c'_{\delta} + \sum_j \left( -\frac{1}{2} \sqrt{\frac{\delta_j}{a_j}} c_{\delta-1_j} + \frac{1}{2} \sqrt{\frac{\delta_j+1}{a_j}} c_{\delta+1_j} \right) a'_j \tag{3.36}$$

where  $\delta \pm 1_j$  is just  $[\delta_1, \dots, \delta_j \pm 1, \dots, \delta_D]$ . Once  $a' = [a'_1, \dots, a'_j, \dots, a'_D]$  has been prescribed, it is straightforward to combine (3.36) and the right hand side of (3.27) to produce equations for the derivatives of the coefficients.

We have seen in Section 3.3 that it is difficult to exactly find the best value of  $a$  to represent the solution  $p$ . Once a sufficiently good value has been determined, however,

Algorithm 3.1:

- 
1. Compute  $c'_\delta$  by assembling (3.27).
  2. Determine the derivative of the expectation value according to the coefficients just computed and let  $a'$  take this value;  $a'_j \equiv (x_j, \partial/\partial t p(\cdot, t))$ .
  3. Account for the dynamic basis by updating  $c'_\delta$  according to (3.36).
- 

it seems natural from the discussion in Section 3.3 to dynamically update  $a$  with the expectation value. Suppose therefore that a good choice of  $a(t=0)$  has been made so that  $p(\cdot, t=0)$  is efficiently represented. Then we define  $a'(t)$  for  $t \geq 0$  by the derivative of the expectation value and obtain Algorithm 3.1.

In practice we also enforce  $a \geq 1$  since Theorem 3.1 is uniform under this restriction. The usefulness of this technique is demonstrated in Section 4.3

To conclude this section we finally comment on the mass-preserving issue since we have actually only discussed how to form the  $l^2$ -projection  $\hat{\pi}_N$ . The reason for this is that forming  $\hat{\pi}_N^0$  follows as a corollary: simply compute the derivative of the mass under  $\hat{\pi}_N$ , then update the lowest order derivative  $c'_0$  so that the resulting coefficients carry a stationary mass. In the case of a stationary parameter  $a$  this amounts to simply summing the ansatz (3.26) over all the integers using a suitable Gauss-Charlier quadrature. When the parameter is dynamic one proceeds in a similar fashion although this time one has to compute the derivative of the mass according to the slightly more involved expression (3.34).

In summary it is a straightforward (but not trivial) task to write general software using the suggested scheme. Inputs include the reactions  $(w_r, \mathbb{N}_r)$  and a *reaction topology* to help sorting out the dependence between the dimensions. After forming a suitable initial distribution, any ODE-solver (explicit or implicit) can be used to evolve the coefficients in a time-dependent setting. Alternatively, an iterative linear or nonlinear solver can be used in the case of a steady-state formulation. The dynamic parameter  $a$  helps capture solutions which vary over many scales in time, but a static parameter is usually preferable for steady-state solutions.

## 4 Numerical experiments

We will now demonstrate the feasibility of the proposed method by numerically solving three different models. The first is a one-dimensional model problem with known solution and is used to demonstrate the application of the theory and the numerical convergence. The second model is four-dimensional with two metabolites and two enzymes, and the task is to find the steady-state distribution. By contrast, the third model is dynamic and takes place in two dimensions only. Here, the behavior of the solution is more complicated and the example provides a setting for which the deterministic reaction-rate

approach fails. The section concludes with a discussion of efficiency and a comparison with Monte-Carlo simulations.

#### 4.1 Convergence and application of the theory

As a numerical demonstration of convergence and in order to highlight the application of the theory in Section 3.1 we first consider the linear birth-death problem (2.12) with time-dependent solution given by (2.15).

To see how the theory of Section 3.1 fit in this case we first note that the master operator in (2.13) is bounded when regarded as an operator  $h^{m+2} \rightarrow h^m$ , which follows immediately from Propositions 3.1 and 3.2. In order to complete a strict convergence proof of the scheme, we need stability and a regularity estimate of the solution. The former issue was discussed in Section 3.2 and we therefore proceed under the assumption of stability. In the present case the regularity is immediate since we do know the exact solutions. To generally determine conditions on the master operator in  $D$  dimensions for a certain given degree of regularity of the solution seems difficult, even in steady-state.

The experiments were conducted as follows. We let the parameters be defined by  $[k, \mu] = [1, 10^{-3}]$  in (2.12) which makes the expectation value in steady-state to be  $m = 1000$ . At  $t=0$ , the initial data is set to a Poisson distribution with mean 10 and the system is then evolved until  $t=10^4$ . By comparing the solution thus obtained to the exact solution (2.15), the time-averaged error was determined. A dynamic parameter  $a$  was used to help the basis functions follow the solution as explained in Section 3.4. The method would not have worked without this feature since the solution varies over many scales.

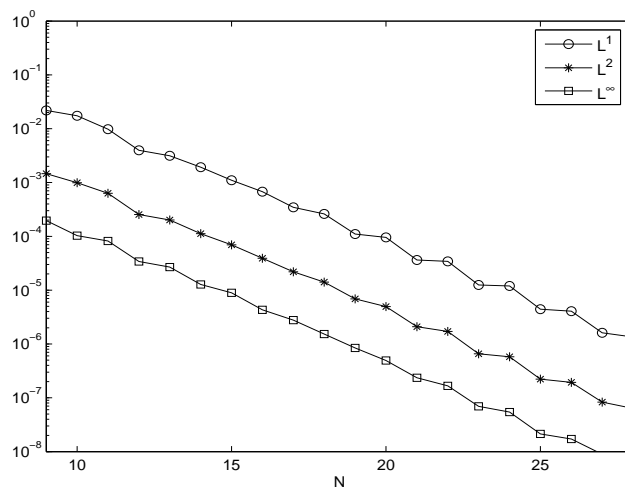
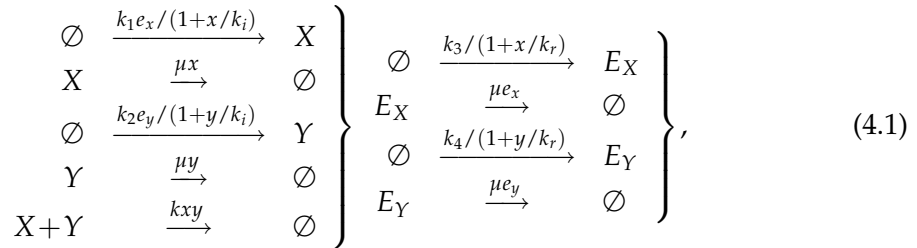


Figure 2: Time-average error of the scheme applied to (2.12) in different norms.

In Fig. 2, errors in various measures are shown and it is clear that the convergence is exponential in the order  $N$  of the scheme. We now proceed to confirm this type of convergence for two more realistic models where no explicit solutions are available.

### 4.2 Enzyme-control of metabolites

This example comes from [14] and is a model of the synthesis of two metabolites  $X$  and  $Y$  by two enzymes  $E_X$  and  $E_Y$ . The reactions are



with parameters  $k_1 = k_2 = 0.3$ ,  $k_3 = k_4 = 0.02$ ,  $k = 10^{-3}$ ,  $\mu = 2 \cdot 10^{-3}$ ,  $k_i = 60$  and  $k_r = 30$ . As it stands, (4.1) is the result of an *adiabatic* [20, Ch. 6.4] simplification of a more complete model. This is generally done by eliminating intermediate products under the assumption that they rapidly reach steady-state.

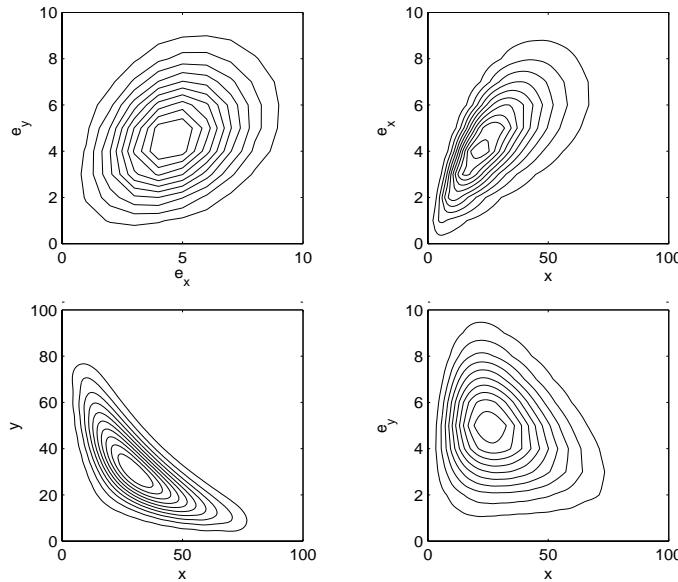


Figure 3: Steady-state solution (marginal distributions) to (4.1). The correlation between the various species can be understood from first principles, except perhaps for the somewhat irregular dependence between  $X$  and  $E_Y$ .

The steady-state solution as obtained by the scheme is displayed in Fig. 3. We have tried several different discretizations with the constant value  $a = [20, 20, 2, 2]$  as a reasonable parameter for the basis. The solution was obtained by explicit time-stepping from initial data in the form of a Poisson distribution with the expectation value  $a$  and steady-state was reached approximately at  $T = 1500$ . The obtained solution is visually pleasing and free of numerical artifacts already at the quite coarse discretization  $[15, 15, 8, 8]$  (degrees per dimension according to the ordering  $[x, y, e_x, e_y]$ ) and took about 9 minutes of

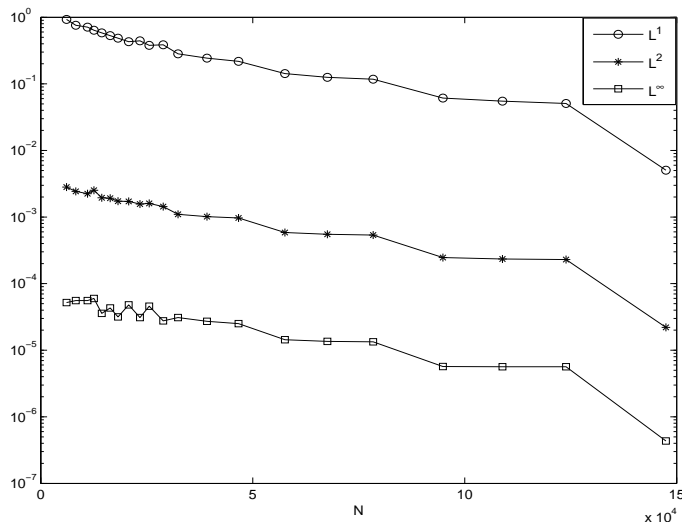
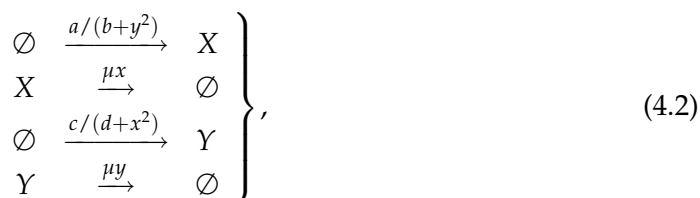


Figure 4: Errors of the scheme applied to (4.1) as measured in different norms. Note that the x-axis displays the total number of degrees of freedom.

computing time on a workstation to obtain. By comparing each solution to a higher order reference solution, different norms of the error were computed and the result is displayed in Fig. 4, where the exponential convergence is reasonably explicit.

### 4.3 Bistable toggle switch

A biological *toggle switch* can be formed by two mutually cooperatively repressing gene products X and Y [21]. The relevant equations are



with parameters  $a = c = 1000$ ,  $b = d = 6000$  and  $\mu = 10^{-3}$ . It is easy to get a rough feeling for the behavior of (4.2). Suppose that initially, the number of X-molecules is large and that the number of Y-molecules is small. Then we see that the production of Y-molecules is inhibited so that the system will find a stable state with  $x > y$ . However, by a certain small probability the stochastic noise can make the number of Y-molecules eventually grow. Due to this 'tunneling' effect, the production of X-molecules will instead be inhibited and the roles of X and Y may suddenly switch. This behavior is explicitly seen in Fig. 5 where the result of a stochastic simulation with SSA [23] is displayed.

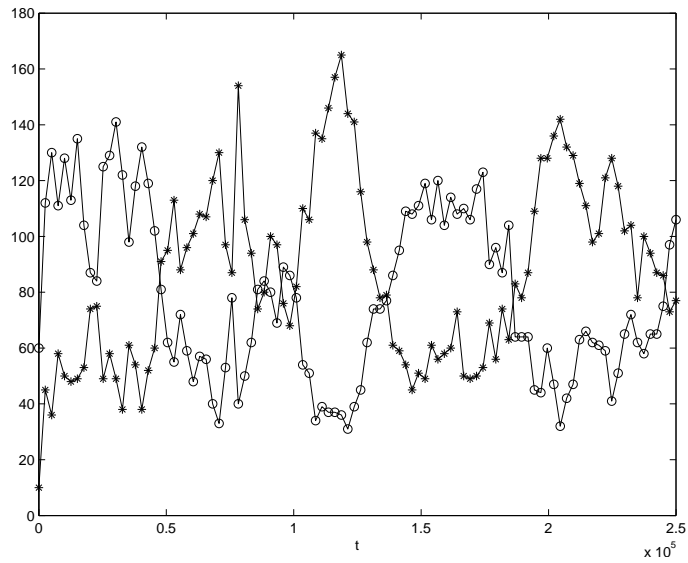


Figure 5: One realization of (4.2) obtained by Gillespie's algorithm. In this simulation the system 'switches' three times and we also see a 'near-switch' slightly before  $t = 10^5$ .

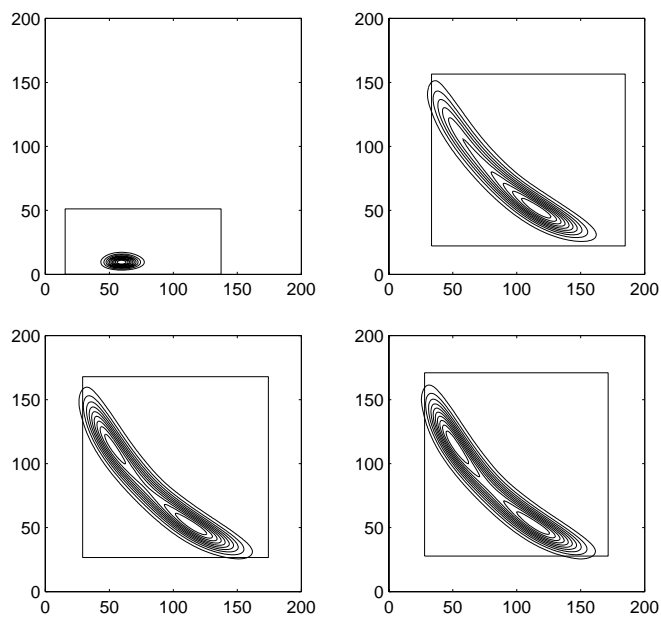


Figure 6: The solution to (4.2) at time  $t = [0, 1, 1.5, 2.5] \cdot 10^5$  using  $N = 19$  (400 coefficients). The simulation starts with a Poissonian solution centered at  $(x, y) = (60, 10)$  and ends in equilibrium where two distinct peaks have formed. The indicated bounding box contains all quadrature points and follows the solution quite well. Note the stiffness of the problem: the fast scale is the transport along the line  $x - y = \text{constant}$ , while the slow distribution along  $x \cdot y = \text{constant}$  is much more of diffusive character.

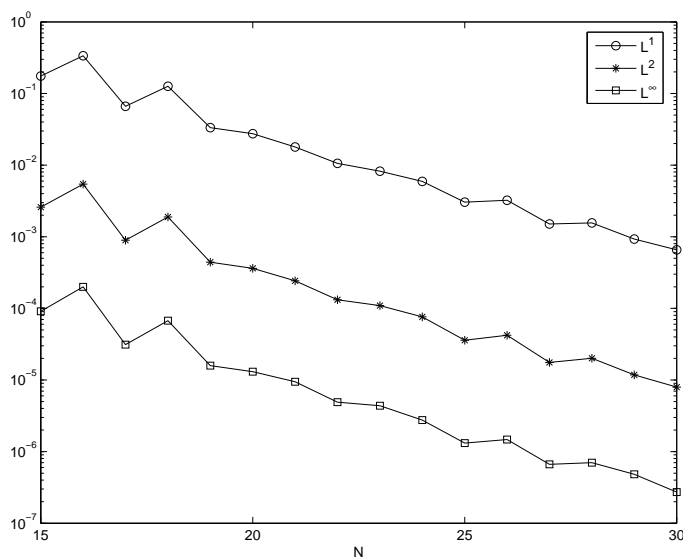


Figure 7: Errors of the scheme applied to (4.2) in different norms (time-average) for increasing order  $N$ . The exponential convergence of the method is clearly visible.

We solved (4.2) using various order  $N$  and various initial data. The parameter  $a$  was dynamic and followed the expectation value of the solution as explained in Section 3.4. The stiffness of the problem is clearly visible in Fig. 6, and so an implicit ODE-solver has been our preferred choice (we used MATLAB's `ode15s`).

The error has been estimated using a high order reference solution with stricter tolerances for the time-stepper. In Fig. 7 several different norms of the error are displayed and the exponential convergence of the method is clearly visible. Fig. 6 indicates a visually pleasing result already at a quite coarse discretization — the solution displayed takes about a minute of computing time on a workstation to obtain. Overall, no problems of instabilities were ever encountered although phase errors were more pronounced for small  $N$ .

The formation of two distinct peaks is an interesting feature which makes the toggle switch an example for which the reaction-rate approach must fail. The expectation value obtained using this method comes to rest near one of the two peaks with an additional unstable critical point situated in between them. The 'switching' feature of the system is thus not present and the deterministic solution provides limiting insight.

#### 4.4 Discussion

Although a complete discussion of spectral methods versus Monte-Carlo simulations is beyond the scope here, we offer some comments of relevance to the examples presented. First, note that *directly* representing the solution in either one of Fig. 3 or 6 is about 100 times more memory consuming than the method proposed.

It is not a well-defined task to compare a spectral method to a Monte-Carlo simulation since they produce different information: the density contains *all* trajectories but contains no concept of individuality. If we agree to look at the error in moment only, the error  $\epsilon$  of the spectral method satisfies

$$\epsilon \sim \exp(-N^{1/D}) \quad (4.3)$$

for  $N$  modes in  $D$  dimensions. The work for obtaining this error becomes in an idealized case  $W \sim N \sim (-\log \epsilon)^D$ , whereas for a Monte-Carlo method the work is the familiar  $W \sim \epsilon^{-2}$ . Thus, for not too high dimensionality and sufficient accuracy demands, the proposed method will be more efficient.

On the other hand, for more than (say) 6 dimensions and/or when only a rough estimate of the average behavior is sufficient, the full spectral solution is probably overkill. This is also often true for non-stiff models where a direct simulation wastes little or no time in resolving fast transients. For stiff problems, however, more complicated model reduction techniques has to be employed and obtaining precise information from the given model becomes more expensive. For the spectral method, a suitably tuned implicit solver can be used so that the time-step restriction is much less severe.

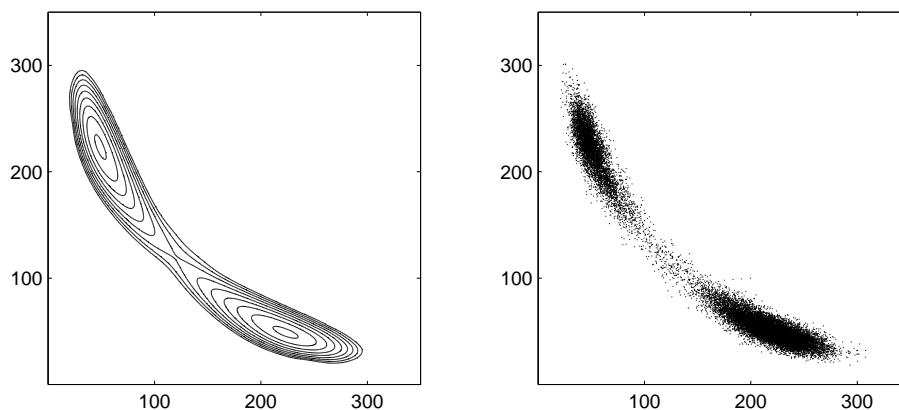


Figure 8: Steady-state solution to (4.2) with parameters  $a = c = 3000$ ,  $b = d = 11000$  and  $\mu = 10^{-3}$  [44]. The problem starts at  $t=0$  in the lower right state and steady-state is approximately reached at  $t=5 \cdot 10^6$ . Left: the result of the spectral method of order 39 (1600 coefficients), contour levels  $4 \cdot 10^{-4} \cdot 2^{-i}$  for  $i=0, \dots, 8$ . Right: one single trajectory simulated using SSA. Note that the system switches only two times during the simulation and that the computational cost for obtaining the solutions displayed is about the same.

One also has to take the various implementation constants into account. Consider as an example of this the bistable system with parameters chosen as in [44] (see Fig. 8). For this particular example, a single simulated trajectory is just about as expensive to compute as a highly accurate spectral representation of the solution to the CME (5 minutes on a workstation for solving the CME and 4 minutes for the single trajectory displayed in Fig. 8). A word of caution when comparing computing times seems to be in order here: our MATLAB implementation is experimental and relies completely on the suite of

included ODE-solvers. It is very likely that a better implementation in a compiled language with a specially adapted time-stepper would improve performance drastically. On the other hand, we have also used a straightforward MATLAB implementation of SSA and similar improvements are possible here. Refer to [36] for further comparisons and connections between solving the CME and obtaining samples via the SSA and the tau-leap methods.

We finally wish to emphasize that the proposed method is not to be regarded foremost as an alternative to Monte-Carlo simulations. Methods for simulating realizations of a system and computing its probability density are not mutually exclusive and are effective in answering different kinds of questions.

## 5 Conclusions

Relying on the Markov assumption only, the master equation is a stochastic description of general time-continuous systems expressed in discrete coordinates, particularly suitable as a description of well-stirred chemically reacting systems. If the number of molecules is large, then an effective and usually accurate description in terms of deterministic ODEs for the expectation values can be formed. However, stochastic descriptions are preferred for many systems of interest; important examples can be found inside living cells where the effects of stochasticity are critical.

Monte-Carlo simulations such as Gillespie's SSA are effective in computing single trajectories, but the solution obtained in terms of the full probability density function can provide additional insight. Statistical parameters can be accurately determined, certain inverse problems are made feasible or can be solved to greater accuracy, and the exact nature of the processes involved can be studied more closely.

We have implemented and applied a spectral method for the master equation based on Charlier functions. Features include high accuracy at a fairly low resolution per dimension, convergence properties in the full semi-infinite discrete state-space, and a strategy for dynamically keeping the basis functions adjusted to the solution they represent. The numerical experiments suggest that the scheme is effective for high enough accuracy demands and not too high dimensionality.

Although the dimensional curse is still an issue, the exponential convergence makes the proposed spectral expansion much more effective than a direct representation. We also would like to point out that the master equation encompasses a very broad class of problems and no single solution method can be optimal in all settings. — The "curse" is a genuine one and cannot be addressed without extra assumptions or reductions to the physical model.

After this work was completed, the author became aware of a similar method for polyreaction kinetics devised by Deuflhard and Wulkow [9,47,48]. Their original scheme uses the basis  $\{\tilde{C}_n^a(x)\} := \{C_n^a(x) \cdot w(x)\}$  and determines the coefficients by taking the  $l^2$ -product with  $\{C_n^a(x)\}$  in a Petrov-Galerkin formulation. The setting is one-dimensional

and the model problem treated is reminiscent of the birth-death problem (2.12). However, when applied to the CME of dimensionality higher than one, their scheme does not seem to be stable with the method of lines discretization. A related recent work directly aimed at the CME is found in [8, Report].

We can also relate the method to the *Poisson representation* [20, Ch. 7.7] which assumes that the solution to the master equation can be written as a superposition of multivariate uncorrelated Poisson distributions:

$$p(x,t) = \int f(a,t) \frac{a^x}{x!} e^{-a} da. \quad (5.1)$$

It is possible to cast the CME into an explicit equation for the new unknown density  $f$ , thereby mapping the CME in  $(x,t)$ -space into a partial differential equation in  $(a,t)$ -space. Note, however, that the relation (5.1) may well imply an arbitrarily peaky and discontinuous  $f$  from a fairly smooth  $p$  (e.g.  $f$  is a Dirac-function for the simple model-problem (2.12)). This observation suggests that perhaps the Poisson representation is better thought of as a tool for deriving various analytical results rather than as a numerical method.

We would also like to mention some possible improvements to the proposed method. First, for certain problems the solution may become a very flat distribution. The proposed basis is really only an effective representation when the essential support of the solution is clustered around the expected value  $m$  as  $m \pm \mathcal{O}(\sqrt{m})$ . If this condition is violated so that the solution is very non-Poissonian, a very high order  $N$  is needed in order to resolve the problem. A cure is to *scale* the solution appropriately which for a discrete solution amounts to incorporating *aggregation*. Aggregation of continuous-time Markov chains has been described in [28] and in the setting of the sparse grids technique for the master equation in [29].

Another improvement would stem from coupling the described method to the reaction-rate equations. One is frequently interested in the precise behavior of the solution in a few dimensions only and the representation in terms of expectation values might well suffice for the major part. A drastic efficiency gain is thus possible, making really high dimensional problems tractable. Some steps in this direction for the Fokker-Planck equation have been taken in [35].

## Acknowledgments

Many comments and suggestions by Per Löstedt have improved the content of this paper. Various inputs from Jan Hesthaven, Stephen Lau and Andreas Hellander were helpful during the final stages of writing and Henrik Hult helped in sorting out the dependence of Theorem 2.1 on the contractivity of the corresponding semigroup. The author is also indebted to Hermann Matthies for a long and valuable discussion during the IHP-EU Workshop "Breaking Complexity" in Bad Honnef, Germany. References [8, 9, 47, 48] was

kindly provided to the author by Peter Deuflhard and Michael Wulkow. Financial support has been obtained from the Swedish National Graduate School in Mathematics and Computing.

## References

- [1] M. Abramovitz and I.A. Stegun. *Handbook of Mathematical Functions*. Dover, New York, 1970.
- [2] D. F. Anderson. Incorporating postleap checks in tau-leaping. *J. Chem. Phys.*, 128(5):054103–054111, 2008. doi:10.1063/1.2819665.
- [3] W. J. Anderson. *Continuous-Time Markov Chains*. Springer Series in Statistics. Springer-Verlag, New York, 1991.
- [4] B. C. Berndt. *Ramanujan’s Notebooks, Part I*. Springer-Verlag, New York, 1985.
- [5] K. Burrage, M. Hegland, F. Macnamara, and B. Sidje. A Krylov-based finite state projection algorithm for solving the chemical master equation arising in the discrete modelling of biological systems. In A. N. Langville and W. J. Stewart, editors, *Markov Anniversary Meeting: An international conference to celebrate the 150th anniversary of the birth of A. A. Markov*, pages 21–38. Bosc Books, Raleigh, NC, USA, 2006.
- [6] Y. Cao, D. Gillespie, and L. Petzold. Multiscale stochastic simulation algorithm with stochastic partial equilibrium assumption for chemically reacting systems. *J. Comput. Phys.*, 206:395–411, 2005. doi:10.1016/j.jcp.2004.12.014.
- [7] Y. Cao, L. R. Petzold, M. Rathinam, and D. T. Gillespie. The numerical stability of leaping methods for stochastic simulation of chemically reacting systems. *J. Chem. Phys.*, 121(24):12169–12178, 2004. doi:10.1063/1.1823412.
- [8] P. Deuflhard, W. Huisinga, T. Jahnke, and M. Wulkow. Adaptive discrete Galerkin methods applied to the chemical master equation. Technical Report 07-04, Zuse Institute Berlin, 2007. <http://www.zib.de/bib/pub>.
- [9] P. Deuflhard and M. Wulkow. Computational treatment of polyreaction kinetics by orthogonal polynomials of a discrete variable. *IMPACT Comp. Sci. Eng.*, 1(3):269–301, 1989. doi:10.1016/0899-8248(89)90013-X.
- [10] T. M. Dunster. Uniform asymptotic expansions for Charlier polynomials. *J. Approx. Theory*, 112:93–133, 2001. doi:10.1006/jath.2001.3595.
- [11] E. B. Dynkin. *Markov processes, volume I*. Academic Press, 1965.
- [12] W. E, D. Liu, and E. Vanden-Eijnden. Nested stochastic simulation algorithm for chemical kinetic systems with disparate rates. *J. Chem. Phys.*, 123(19), 2005. doi:10.1063/1.2109987.
- [13] J. Elf and M. Ehrenberg. Spontaneous separation of bi-stable biochemical systems into spatial domains of opposite phases. *Syst. Biol.*, 1(2):230–236, 2004. doi:10.1049/sb:20045021.
- [14] J. Elf, P. Lötstedt, and P. Sjöberg. Problems of high dimension in molecular biology. In W. Hackbusch, editor, *Proceedings of the 19th GAMM-Seminar in Leipzig “High dimensional problems - Numerical Treatment and Applications”*, pages 21–30, 2003.
- [15] S. Engblom. Computing the moments of high dimensional solutions of the master equation. *Appl. Math. Comput.*, 180(2):498–515, 2006. doi:10.1016/j.amc.2005.12.032.
- [16] S. Engblom. Gaussian quadratures with respect to discrete measures. Technical Report 2006-007, Dept of Information Technology, Uppsala University, Uppsala, Sweden, 2006. <http://www.it.uu.se/research>.

- [17] S. Engblom. A discrete spectral method for the chemical master equation. Technical Report 2008-005, Dept of Information Technology, Uppsala University, Uppsala, Sweden, 2008. <http://www.it.uu.se/research>.
- [18] L. Ferm and P. Lötstedt. Adaptive solution of the master equation in low dimensions. Appl. Numer. Math, In Press, Corrected Proof, 2008.
- [19] L. Ferm, P. Lötstedt, and P. Sjöberg. Conservative solution of the Fokker-Planck equation for stochastic chemical reactions. BIT, 46:S61–S83, 2006. doi:10.1007/s10543-006-0082-z.
- [20] C. W. Gardiner. Handbook of Stochastic Methods. Springer Series in Synergetics. Springer-Verlag, Berlin, 3rd edition, 2004.
- [21] T. S. Gardner, C. R. Cantor, and J. J. Collins. Construction of a genetic toggle switch in *Escherichia coli*. Nature, 403:339–342, 2000. doi:10.1038/35002131.
- [22] B. Gaveau, M. Moreau, and J. Toth. Master equation and Fokker-Planck equation: Comparison of entropy and of rate constants. Letters in Math. Phys., 40(2):101–115, 1997.
- [23] D. T. Gillespie. A general method for numerically simulating the stochastic time evolution of coupled chemical reactions. J. Comput. Phys., 22(4):403–434, 1976. doi:10.1016/0021-9991(76)90041-3.
- [24] D. T. Gillespie. A rigorous derivation of the chemical master equation. Physica A, 188:404–425, 1992. doi:10.1016/0378-4371(92)90283-V.
- [25] D. T. Gillespie. Approximate accelerated stochastic simulation of chemically reacting systems. J. Chem. Phys., 115(4):1716–1733, 2001. doi:10.1063/1.1378322.
- [26] P. Guptasarama. Does replication-induced transcription regulate synthesis of the myriad low copy number proteins of *Escherichia coli*? Bioessays, 17(11):987–997, 1995. doi:10.1002/bies.950171112.
- [27] E. L. Haseltine and J. B. Rawlings. Approximate simulation of coupled fast and slow reactions for stochastic chemical kinetics. J. Chem. Phys., 117(15), 2002. doi:10.1063/1.1505860.
- [28] M. Haviv. Aggregation/disaggregation method for computing the stationary distribution of a Markov chain. SIAM J. Numer. Anal., 24(4):952–966, 1987. doi:10.1137/0724062.
- [29] M. Hegland, C. Burden, L. Santoso, S. MacNamara, and H. Booth. A solver for the stochastic master equation applied to gene regulatory networks. J. Comput. Appl. Math., 205(2):708–724, 2007. doi:10.1016/j.cam.2006.02.053.
- [30] J. S. Hesthaven, S. Gottlieb, and D. Gottlieb. Spectral Methods for Time-Dependent Problems. Cambridge Monographs on Applied and Computational Mathematics. Cambridge University Press, Cambridge, 2007.
- [31] N. G. van Kampen. Stochastic Processes in Physics and Chemistry. Elsevier, Amsterdam, 5th edition, 2004.
- [32] R. Koekoek and R. F. Swarttouw. The Askey-scheme of hypergeometric orthogonal polynomials and its  $q$ -analogue. Technical Report 98-17, Dept. of Technical Mathematics and Informatics, Delft University of Technology, 1998. <http://aw.twi.tudelft.nl/~koekoek/askey.html>.
- [33] T. Li. Analysis of explicit tau-leaping schemes for simulating chemically reacting systems. Multiscale Model. Simul., 6(2):417–436, 2007. doi:10.1137/06066792X.
- [34] T. Li, A. Abdulle, and W. E. Effectiveness of implicit methods for stiff stochastic differential equations. Commun. Comput. Phys., 3(2):295–307, 2008.
- [35] P. Lötstedt and L. Ferm. Dimensional reduction of the Fokker-Planck equation for stochastic chemical reactions. Multiscale Model. Simul., 5:593–614, 2006.
- [36] S. MacNamara, K. Burrage, and R. B. Sidje. Multiscale modeling of chemical kinetics via the master equation. Multiscale Model. Simul., 6(4):1146–1168, 2008. doi:10.1137/060678154.

- [37] H. G. Matthies and A. Keese. Galerkin methods for linear and nonlinear stochastic partial differential equations. *Comput. Methods Appl. Mech. Engrg.*, 194(12–16):1295–1331, 2005. doi:10.1016/j.cma.2004.05.027.
- [38] B. Munsky and M. Khammash. The finite state projection algorithm for the solution of the chemical master equation. *J. Chem. Phys.*, 124(4):044104, 2006. doi:10.1063/1.2145882.
- [39] F. W. J. Olver. *Asymptotics and Special Functions*. Academic Press, New York, 1974.
- [40] M. Rathinam, L. Petzold, Y. Cao, and D. T. Gillespie. Stiffness in stochastic chemically reacting systems: The implicit tau-leaping method. *J. Chem. Phys.*, 119(24):12784–12794, 2003. doi:10.1063/1.1627296.
- [41] M. Rathinam, L. R. Petzold, Y. Cao, and D. T. Gillespie. Consistency and stability of tau-leaping schemes for chemical reaction systems. *Multiscale Model. Simul.*, 4(3):867–895, 2005. doi:10.1137/040603206.
- [42] M. S. Samoilov and A. P. Arkin. Deviant effects in molecular reaction pathways. *Nature Biotech.*, 24:1235–1240, 2006. doi:10.1038/nbt1253.
- [43] J. Shen. Stable and efficient spectral methods in unbounded domains using Laguerre functions. *SIAM J. Numer. Anal.*, 38(4):1113–1133, 2000.
- [44] P. Sjöberg, P. Lötstedt, and J. Elf. Fokker-Planck approximation of the master equation in molecular biology. *Comp. Vis. Sci.*, To appear, 2008. doi:10.1007/s00791-006-0045-6.
- [45] Y. Togashi and K. Kaneko. Molecular discreteness in reaction-diffusion systems yields steady states not seen in the continuum limit. *Phys. Rev. E*, 70(2):020901–1–020901–4, 2004. doi:10.1103/PhysRevE.70.020901.
- [46] J. M. G. Vilar, H. Y. Kueh, N. Barkai, and S. Leibler. Mechanism of noise-resistance in genetic oscillators. *Proc. Nat. Acad. Sci.*, 99:5988–5992, 2002. doi:10.1073/pnas.092133899.
- [47] M. Wulkow. Adaptive treatment of polyreactions in weighted sequence spaces. *IMPACT Comp. Sci. Eng.*, 4(2):153–193, 1992. doi:10.1016/0899-8248(92)90020-9.
- [48] M. Wulkow. The simulation of molecular weight distributions in polyreaction kinetics by discrete Galerkin methods. *Macromol. Theory. Simul.*, 5(3):393–416, 1996. doi:10.1002/mats.1996.040050303.
- [49] D. Xiu and J. S. Hesthaven. High-order collocation methods for differential equations with random inputs. *SIAM J. Sci. Comput.*, 27(3):1118–1139, 2005. doi:10.1137/040615201.
- [50] D. Xiu and G. E. Karniadakis. The Wiener-Askey polynomial chaos for stochastic differential equations. *SIAM J. Sci. Comput.*, 24(2):619–644, 2002. doi:10.1137/S1064827501387826.